On shear-layer instability, breakdown and transition

By H. P. GREENSPAN AND D. J. BENNEY
Mathematics Department, Massachusetts Institute of Technology

(Received 2 July 1962)

The problem of the linear stability of a time-dependent shear flow is investigated and the effects of contraction and expansion of the layer are discussed. Models of flows observed prior to breakdown are constructed and used to investigate the resulting secondary instabilities which are shown to be extremely violent and in essential agreement with recent experiments. In relatively short time, one half period of the primary oscillation, the energy in the secondary disturbance increases by two orders of magnitude; the wave-number corresponding to maximum amplification is five times that of the primary wave.

1. Introduction

The recent experiments of Klebanoff, Tidstrom & Sargent (1962) and Kovasznay, Komoda & Vasudeva (1962) concerning transition show that before breakdown occurs an intense shear layer forms within the boundary layer on a flat plate. It appears that the secondary instabilities arising from the shear are responsible for the dramatic sudden changes in the flow which initiate transition.

With this motivation, we have studied an extremely simple model of a class of unbounded time-dependent shear layers and this is presented in § 2. In § 3, the model is adapted to the case of boundary-layer transition; the results of this investigation and those of previous studies provide a more complete (but by no means final) description of the breakdown process.

2. Stability of time-dependent shear layers

Let $\bar{\mathbf{q}} = (\bar{u}(y,t), 0, 0)$ be the vector velocity of a unidirectional incompressible viscous flow. It is well known (Squires theorem) that only the two-dimensional linear stability problem need be considered, in which case the pertinent equation governing the perturbation stream function ψ,

$$\mathbf{q}' = \nabla \times (\psi \hat{\mathbf{i}}_3)$$

is

$$\nabla^2(\nu\nabla^2\psi - \psi_t) - \bar{u}\nabla^2\psi_x + \psi_x \bar{u}_{yy} = 0.$$

Furthermore, if we consider only the inviscid limiting case, and if the disturbance is of the form

$$\psi(x,y,t) = \phi(y,t)\, e^{i\alpha x},$$

then

$$\left(\frac{\partial}{\partial t} + i\alpha\bar{u}(y,t)\right)\left(\frac{\partial^2}{\partial y^2} - \alpha^2\right)\phi - i\alpha\bar{u}_{yy}\phi = 0. \tag{2.1}$$

The general solution may be obtained by superposition or a Fourier integral.

Since the applications of our theory concern flows which are not unidirectional, it seems appropriate to comment upon the basic approach at this time.

Suppose $\bar{\mathbf{q}}(x, y, z, t)$ is a basic flow, known either analytically or experimentally, which resembles a unidirectional shear flow in a certain specific local region of space. If we are interested solely in the instabilities involving waves of small scales arising in this particular neighbourhood, $\bar{u}(y, t)$ may be used in equation (2.1) as a very reasonable local approximation of the real flow. Although the complicated basic flow must satisfy the conservation laws, the simple approximation may not, if it is used solely to circumvent extreme analytical difficulties. In other words, $\bar{u}(y, t)$ is to be interpreted as a simple local analytical description of a known but very complex flow pattern, and not necessarily as a solution of the fundamental equations of motion. (There are few unidimensional solutions, none of which is pertinent in the discussion of § 3.)

A simple approximate (or substitute) flow pattern worthy of consideration because it reduces the stability equation to a tractable form, is the time-dependent shear layer, consisting of the broken-line velocity profiles†

$$\bar{u}(y,t) = \begin{cases} U(t)\, y/|y|, & |y| \geqslant h; \\ U(t)\, y/h(t), & |y| \leqslant h. \end{cases}$$

Here $U(t)$ and $h(t)$ are to be chosen so as to simulate best a known flow in some neighbourhood.

For such profiles, the term $\bar{u}_{yy}$ disappears from the fundamental equation and is accounted for solely by jump discontinuities across the lines $|y| = h(t)$.

It is convenient to introduce, at this time, the dimensionless variables

$$y_* = y/h(0), \quad t_* = U(0)\, t/h(0), \quad \xi = h(t)/h(0),$$
$$\eta = U(t)/U(0), \quad \phi_* = \phi/(h(0)\, U(0)),$$

with $\alpha h(0) = k$. (Henceforth, we drop the asterisk notation.) The complete dimensionless problem is

$$\left(\frac{\partial}{\partial t} + ik\bar{u}\right)\left(\frac{\partial^2}{\partial y^2} - k^2\right)\phi = 0, \tag{2.2}$$

with the boundary conditions

$$\left.\begin{aligned} \lim_{|y|\to\infty} \phi = 0, \quad [\phi]_{\pm\xi} = 0, \\ [(\partial/\partial t + ik\bar{u})\,\phi_y - ik\phi\bar{u}_y]_{\pm\xi} = 0, \end{aligned}\right\} \tag{2.3}$$

where

$$[f(y,t)]_\xi = f(\xi+, t) - f(\xi-, t)$$

and

$$\bar{u} = \begin{cases} \eta(t)\, y/|y|, & |y| \geqslant \xi, \\ \eta(t)\, y/\xi, & |y| \leqslant \xi. \end{cases} \tag{2.4}$$

The initial conditions are chosen to correspond to the modal solutions of the Rayleigh problem, equation (2.10), so that, in actuality, the functions $\xi(t)$, $\eta(t)$ are defined as unity for all negative times. We determine, in this manner, the effects of the subsequent time variations of thickness and velocity on both the stable and unstable classical modal solutions. Of course, a more general initial-

† G. F. Carrier in some unpublished research considered a similar profile in connexion with a shear layer whose thickness increases as $\sqrt{t}$.

value problem can be solved just as easily, but many of the important features of the solution would then be obscured.

The solution of the foregoing problem may be represented as

$$\phi = \begin{cases} d(t)\, e^{-ky}, & y \geqslant \xi; \\ a(t)\, e^{ky} + b(t)\, e^{-ky}, & |y| \leqslant \xi; \\ g(t)\, e^{ky}, & y \leqslant -\xi. \end{cases} \tag{2.5}$$

The time-dependent coefficient functions, which are in general complex functions of a real variable, satisfy

$$\left.\begin{aligned} d(t) &= a(t)\, e^{2k\xi} + b(t), \\ g(t) &= a(t) + b(t)\, e^{+2k\xi}; \end{aligned}\right\} \tag{2.6}$$

$$\left.\begin{aligned} d\Phi/dt &= k\eta F(k\xi(t))\, \theta, \\ d\theta/dt &= k\eta G(k\xi(t))\, \Phi; \end{aligned}\right\} \tag{2.7}$$

where

$$\left.\begin{aligned} a(t) &= \tfrac{1}{2}(\Phi + i\theta)\, e^{-k\xi}, \\ b(t) &= \tfrac{1}{2}(\Phi - i\theta)\, e^{-k\xi}; \end{aligned}\right\} \tag{2.8}$$

and

$$\left.\begin{aligned} 2zF(z) &= e^{-2z} + 2z - 1, \\ 2zG(z) &= e^{-2z} - 2z + 1. \end{aligned}\right\} \tag{2.9}$$

Before we make any general comments about this system of equations, it is advisable to review briefly the classical problem of Rayleigh instability. This, as we have said, corresponds to the choice $\xi = 1$, $\eta = 1$ for all t, so that the solutions of (2.7) are

$$\left.\begin{aligned} \Phi &= \Phi_0\, e^{\pm\sigma t}, \\ \theta &= \Phi (G/F)^{\frac{1}{2}}, \\ \sigma &= \mathrm{Re}\{k(GF)^{\frac{1}{2}}\}, \end{aligned}\right\} \tag{2.10}$$

($\Phi_0 = 1$ is the usual choice). G is a positive or negative function depending on whether k is less than or larger than 0·63925, the cut-off wave-number. One mode is unstable in the former régime and both are neutrally stable in the latter; the amplification factor σ has its maximum value, 0·20, at $k = 0{\cdot}399$.

Carrier (1954) and Esch (1957), in their extensive studies of the classical problem, computed the amplification factor for the continuous hyperbolic tangent profile as well as several piecewise-linear approximations. These studies indicate that the profile of equation (2.4) yields results which are qualitatively and in some respects quantitatively correct; further increase in the number of 'broken' line approximations produce only very minor changes in the maximum amplification factor although the cut-off wave-number increases somewhat (see Esch 1957, figure 2, page 291). The evidence suggests that the simplest profile, consisting of three straight lines, is a very adequate approximation. (The classical Helmholtz stability problem of the vortex sheet yields neither a cut-off wave-number nor a finite maximum amplification rate.)

It is desirable to characterize the amplification factor as the logarithmic derivative of the total energy per wave length

$$A_f = \frac{1}{2\mathrm{E}} \frac{d\mathrm{E}}{dt}, \tag{2.11}$$

where, as it may be shown,

$$\mathrm{E} = \frac{2\pi}{k}\int_{-\infty}^{\infty}\left(|\tilde{v}|^2 + \frac{1}{k^2}|\tilde{v}_y|^2\right)dy, \tag{2.12}$$

and

$$\mathbf{q}'.\hat{\mathbf{i}}_1 = \tilde{u}\,e^{ikx} + \tilde{u}^*\,e^{-ikx},$$

$$\mathbf{q}'.\hat{\mathbf{i}}_2 = \tilde{v}\,e^{ikx} + \tilde{v}^*\,e^{-ikx}$$

(* denotes complex conjugate here). In particular,

$$\Omega A_f = -k[(\Phi\Phi^* - \theta\theta^*)\,d\xi/dt - (\Phi\theta^* + \Phi^*\theta)\,\eta]\,e^{-2k\xi}, \tag{2.13}$$

$$\Omega = \Phi\Phi^* + \theta\theta^* + (\Phi\Phi^* - \theta\theta^*)\,e^{-2k\xi},$$

and

$$\frac{\mathrm{E}(t)}{\mathrm{E}(0)} = \frac{\Phi\Phi^*(1+e^{-2k\xi}) + \theta\theta^*(1-e^{-2k\xi})}{\Phi_0\Phi_0^*(1+e^{-2k}) + \theta_0\theta_0^*(1-e^{-2k})}. \tag{2.14}$$

The extended definition of amplification factor, in the case of Rayleigh instability, reduces correctly to

$$A_f = \sigma$$

and

$$\mathrm{E}(t) = \mathrm{E}(0)\,e^{2\sigma t}.$$

It is evident, upon inspection of equation (2.7), that the general problem may be reduced to the case of variable shear thickness but constant shear velocity through use of the new independent time variable

$$\tau = \int_0^t \eta(t')\,dt'.$$

For example, the solution of the particular problem, $\eta(t)$ arbitrary but positive, $\xi = 1$ (variable shear velocity, constant shear thickness) is then immediately determined to be

$$\left.\begin{aligned}\Phi &= \Phi_0\,e^{\pm\sigma\tau},\\ \theta &= \Phi(G/F)^{\frac{1}{2}}.\end{aligned}\right\} \tag{2.15}$$

More generally, if $\bar{u}(y,t) = \eta(t)\,w(y)$, then the original equation (2.1) may be reduced by the same change of variable.

We are mainly interested in the most unstable modes. Unfortunately these occur for wave-numbers of order one, a particularly difficult régime to analyze by conventional analytical methods involving perturbation or asymptotic techniques. Other approximation methods based on a single second-order differential equation or the replacement of the complicated functions $F(z)$ and $G(z)$ by simpler forms have been judged inadequate. Our basis approach therefore is direct numerical integration of the system of differential equations.

However, a general qualitative understanding of the results can be obtained directly from the equations. At early times, $t \sim 0$, the amplification factor is essentially

$$A_f \simeq \sigma\eta(t) - (k - \tfrac{1}{2})\,d\xi/dt.$$

If, in addition, it is assumed that $[d\xi/dt]_{0+} \neq 0$ ($\eta(0) = 1$), then the amplification factor is obviously reduced (increased) for values $k > \frac{1}{2}$ ($< \frac{1}{2}$) if $\xi'(0+)$ is positive (negative). Thus it is to be expected that for a contracting shear layer the shorter wavelengths are excited and contain more energy than ordinarily possible (for $\xi' = 0$) whereas the reverse is true for the long wavelengths. If the shear layer

expands, the longer wavelengths are stimulated, the shorter, somewhat suppressed. A sufficiently rapid process will actually suppress certain wavelengths by removing energy and accentuate others by supplying energy. The calculations show this conclusion to be generally true throughout the process.

A perturbation expansion for values $k \ll 1$, $\eta(t) = 1$, leads to the formulas

$$\left.\begin{aligned} \Phi &= \Phi_0\left\{1 + k\int_0^t \xi(t)\,dt + \ldots\right\}, \\ \theta &= \Phi_0\left\{\frac{1}{k} + \int_0^t \frac{dt}{\xi(t)} + \ldots\right\}, \\ \mathrm{E} &= \frac{\mathrm{E}(0)}{1+k}\left\{\xi + k\left(1 + 2\xi\int_0^t \frac{dt}{\xi}\right) + \ldots\right\}. \end{aligned}\right\} \tag{2.16}$$

These results also support the aforementioned conclusion by showing that for small wave-numbers at least, E and ξ increase or decrease together.

An asymptotic theory, for $k \gg 1$, leads to

$$\left.\begin{aligned} \Phi &\sim \Phi_0 \exp\left(-ik\left[t - \frac{1}{2k}\int_0^t \frac{dt}{\xi} + \ldots\right]\right), \\ \theta &\sim -i\Phi, \quad \mathrm{E} \sim \mathrm{E}_0, \quad A_f \sim 0, \end{aligned}\right\} \tag{2.17}$$

which to this order in $1/k$ is not particularly instructive. Neither of the foregoing analyses resulting in equations (2.16) and (2.17) enable us to penetrate the interesting wave-number régime, and further minor results obtained by similar procedures are omitted here in the interests of brevity.

A quasi-stationary approach, seemingly appropriate for slow processes, can be based on the approximate formula for the energy,

$$\mathrm{E} \simeq \mathrm{E}_0 \exp\left\{2\int_{t_s}^t \frac{\eta(t)}{\xi(t)}\sigma(t)\,dt\right\} \tag{2.18}$$

with $$\sigma(t) = Re\{k\xi[F(k\xi)\,G(k\xi)]^{\frac{1}{2}}\}.$$

The lower limit of integration, t_s, is either zero or that time when the function $\sigma(t)$ first becomes zero, whichever is larger. The integration can be performed by further approximating the integrand with some simple rational function. The entire calculation is as tedious and laborious as the direct numerical integration of the relevant equations—and more uncertain. We have, however, made this calculation in the case of boundary-layer transition, and this is reported in the next section.

A series of numerical calculations were performed and the results, which almost speak for themselves, are presented in figures 1–3. Although the computations were made for arbitrary profiles, only a few of the most typical are presented. Some general features do warrant further comment.

Several graphs, for cases of collapsing shear layers, indicate the development of a second energy peak (figure 3). This may be explained by noting that the shear starts from an unstable configuration which already has a wave-number corresponding to maximum amplification. For some time, the mode with this wave-number (or one very nearby), continues to be amplified, and is able to maintain

its maximum energy content. However, as the shear layer contracts, the wave-number of maximum amplification shifts rapidly and decidedly through the original cut-off position. If enough time elapses, another mode appropriate to a new shear thickness replaces the first as the carrier of maximum total energy. The sharp changes in amplification factor in the neighbourhood of the initial cut-off wave-number maintain the original mode as a local maximum.

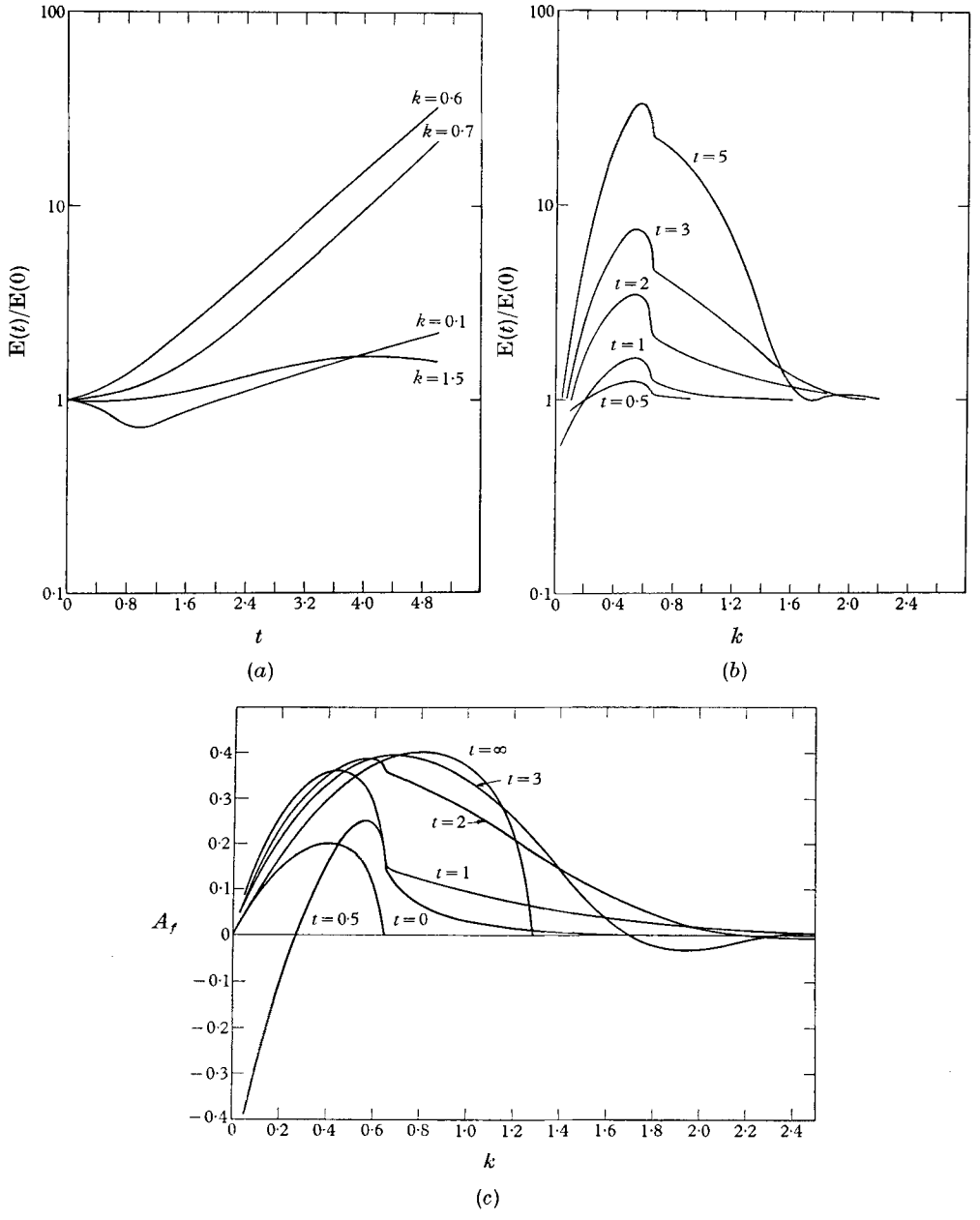

FIGURE 1. Collapsing cubic: $\eta = 1$; $\xi = 1 - (\frac{3}{2} - t)\, t^2$, $0 \leqslant t \leqslant 1$; $\xi = \frac{1}{2}$, $t > 1$. These graphs show $E(t)/E(0)$ and A_f as functions of k and t.

The process of 'shear-layer contraction' acts very much like a frequency or wavelength selector as well as an amplifier. All short wavelengths are amplified, all very long wavelengths suppressed; the wave-number corresponding to maximum amplification generally moves to the right of the corresponding value in the Rayleigh problem. The exact quantitative details depend on the particular process and time histories involved. A similar (reversed) description holds for the expanding layer.

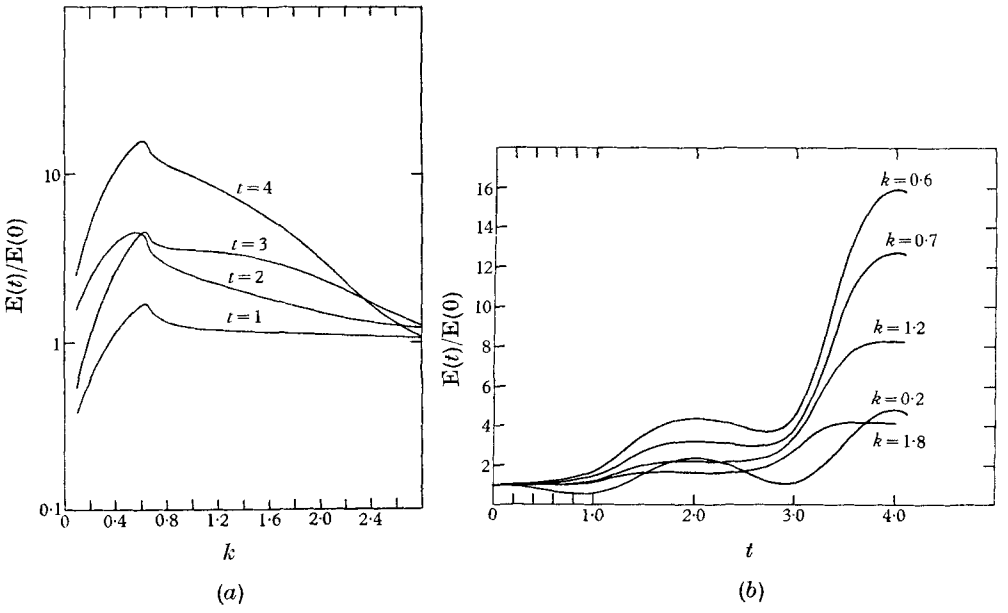

FIGURE 2. Oscillating shear $\xi = 0{\cdot}6 + 0{\cdot}4\cos\pi t$, $\eta = 0{\cdot}5(1-\cos\pi t)$. Graphs show dependence of $E(t)/E(0)$ on k and t.

In cases of rapid collapse, very large amplification factors are noted. However, the short duration of such processes imply a total energy input usually not more than twice the original value. The substantial changes in amplification factor are somewhat illusory in this respect, and the significance of this factor should be discounted somewhat. The parameter which emerges from this analysis as most significant, regarding the effects induced by the time variations, is the energy ratio $E(t)/E(0)$. This factor, a function of time and wave-number, provides a great deal of the information desired about a particular process.

A survey of all the results indicates that $\eta(t)$, the shear velocity, is the most important single factor controlling the total energy amplification whereas $\xi(t)$, the shear layer thickness, has the prime responsibility for selecting the wave-number corresponding to this maximum gain. In addition, the time variation of shear-layer thickness imparts additional amplification to certain modes while it suppresses others.

We now proceed to apply these results to a study of boundary-layer transition.

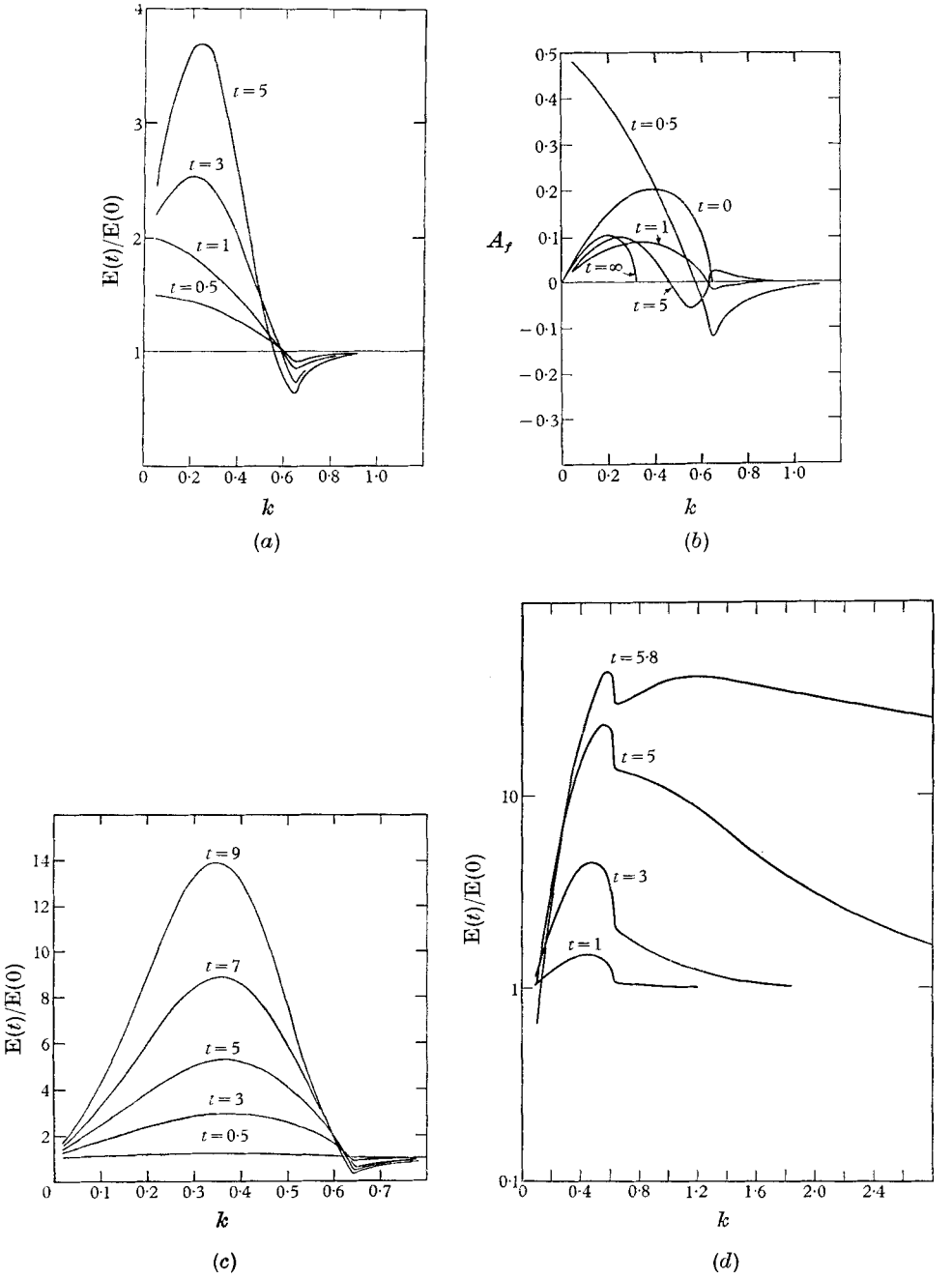

FIGURE 3. (*a*), (*b*) show $E(t)/E(0)$ and A_f as functions of k for an expanding cubic layer; $\eta = 1$; $\xi = 1 + 3(1 - \frac{2}{3}t)\, t^2$ for $0 \leqslant t \leqslant 1$; $\xi = 2$ for $t > 1$. (*c*) shows $E(t)/E(0)$ as a function of k for a parabolic expansion; $\xi = (1 + \frac{1}{10}t)^{\frac{1}{2}}$; $\xi\eta = 1$. (*d*) shows $E(t)/E(0)$ as a function of k for a straight line collapse; $\xi = 1 - \frac{1}{6}t$; $\eta = 1$.

3. Boundary-layer transition

Here we wish to comment on the relevance of the above flow models to the breakdown of the laminar boundary layer. In order to do this it is necessary to review very briefly the known theoretical and experimental facts.

During the initial stages of instability there is excellent agreement between theory (Lin 1945, 1955) and experiment (Schubauer & Skramstead 1948; Schubauer 1957; Klebanoff 1957). Recent developments have centred on the non-linear effects of these wave motions in an effort to carry the theory toward the transition region. The theory proposed by Benney (1961) and Benney & Lin (1960) showed the importance of three dimensionality, a fact strongly indicated by the experiments of Klebanoff *et al.* (1962). A time-dependent analysis has been suggested by Stuart (1960) and Watson (1960), yielding possible finite amplitude equilibrium states of the oscillation. Both of these theories are based on perturbation techniques, and apart from some minor disagreements use essentially the same approach to the problem. The common feature is the modification of the basic flow and the generation of higher harmonics, but neither of these investigations is meaningful beyond the beginning stages of non-linear developments. Thus, the importance of this type of calculation lies in the fact that it gives a qualitative picture of the finite amplitude region necessary as a prerequisite for the sudden breakdown of the flow, rather than a description of the breakdown process itself. Clearly the higher-order perturbations of such theories will add little to answering the question of the dramatic explosion of the flow into the shorter length scales so characteristic of turbulence.

A great deal is to be learned from the carefully controlled experiments of Klebanoff (1962) and Kovasznay *et al.* (1962) who have made detailed measurements at the point of breakdown. One of the most interesting features is the reproducibility of the initial breakdown before the random element takes over. Presumably this is a reflexion of the fact that the initial conditions are so well defined. It is found that the pre-existing finite amplitude effects produce a distinct periodic spanwise variation in the mean flow, associated with a longitudinal vortex structure. Superposed is the eddy system of the primary wave, and at various phases these two systems tend to re-enforce and cancel each other. Up to this point the results are in general agreement with existing theoretical calculations. Breakdown (defined by the occurrence of the first spike) originates as an almost point-like phenomenon corresponding to definite sets of values for x, y, z, t. Evidently the local flow configuration at these positions is such that a new instability arises which is far more violent than the original one. Indeed, in this situation, the possible finite amplitude equilibration of the original instability of the Blasius profile appears to be more of an academic question than a real one, as in practice a new phenomenon soon dominates the system.

An instability analysis of the *new* flow $\mathbf{q}(x, y, z, t)$ caused by finite amplitude effects should resolve this question. While this problem can be formulated very easily, it presents extreme mathematical difficulties in its solution. It is therefore desirable to try to extract the most distinguishing features of this configuration and to use simplified models at a first attempt in any theoretical investigation.

Immediately prior to breakdown there is an intense shear layer formed in the flow once each cycle of the primary wave. This occurs at approximately two-thirds of the boundary-layer thickness and at spanwise positions, corresponding to the so-called 'peaks' of the oscillation. Apparently this local configuration is a direct result of the secondary flow which moves the maximum shear away from the wall (where it is only just unstable), out into the boundary layer where it is extremely unstable. The shear so formed contracts and intensifies as the wave moves downstream. It must be admitted that the formation of this shear layer is accompanied by a three-dimensional stretching of the vortex lines, and the flow is not strictly unidirectional. However, in a local stability analysis the maximum growth rate should be proportional to the maximum local shear, and the latter is still $\partial\bar{u}/\partial y$.

Thus the present state of knowledge consists of the theoretical studies which indicate the formation of the internal shear layers, and of experimental investigations which not only confirm their existence but also serve to determine the manner in which the layers develop. The latter stages of growth are extremely difficult to study analytically. This would have to be done by incorporating still higher-order perturbations in the extension of the linear stability analysis. Since the basic processes involved in the formation of the shear layers are essentially known, and since the extended theory cannot possibly succeed in explaining the mechanism of sudden transition, there seems little point to proceeding in this direction. We can circumvent these analytical difficulties by merely assuming that the basic time-dependent flow pattern is known, as indicated by theory and detailed by experiment. In other words, since the modifications of the original flow by the primary instabilities are understood from the physical as well as theoretical view-points, they are assumed to be known, the details provided by the many excellent experiments. Breakdown, as we see it, is a direct consequence of a new phenomenon, the growth of *secondary* instabilities on a known, but complicated, flow (i.e. the original basic flow modified by the primary instabilities).

In this manner, we can once again utilize the *linear* stability theory of section two to investigate the growth of secondary disturbances in the known flow configuration.

In the neighbourhood of the breakdown position, where the inflexional shear is maximum, the local flow is approximately two dimensional. Figure 4, taken from the work of Kovasznay *et al.* (1962), shows the local behaviour of the modified basic flow. By taking some simple time-dependent approximations of this flow and utilizing the two-dimensional stability theory developed in the preceding section, we can compute the stability characteristics of the secondary disturbances. The results show that the growth of these secondary instabilities correspond in many ways to the sudden burst of high-frequency excitation observed in experiments.

The simplest model of the boundary-layer transition is the unbounded time-dependent shear layer of constant thickness but whose strength varies linearly with respect to the time. The relevant theory was developed in the paragraph including equation (2.15). In order to apply the results we need only determine

the pertinent dimensionless parameters in accordance with the experimental data. Accordingly, reasonable characteristic values to use for velocity and distance (refer to the basic dimensionalization scheme of § 2, preceding equation (2.2)) are

$$U(0) = \tfrac{1}{4}U_f,$$
$$h(0) = \tfrac{1}{10}\delta.$$

In Kovasznay's experiments, the free-stream velocity is $U_f = 1100\,\text{cm/sec}$, $\delta = 0{\cdot}6\,\text{cm}$ is the boundary-layer thickness and $1/T$ or $f = 100\,\text{c/s}$ is the frequency of the primary excitation.

This first model is based upon a dimensionless velocity profile for which, according to equation (2.4),

$$\eta(t) = t/T,$$
$$\xi(t) = 1.$$

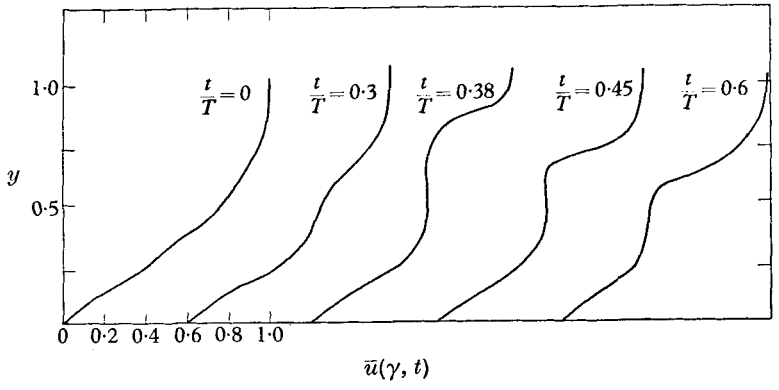

FIGURE 4. Instantaneous velocity profiles at first appearance of a spike; taken from Kovasznay *et al.* (1962). T is the period of the primary wave.

Time is measured from the onset of a shear layer until breakdown which occurs later at approximately half the period of the primary oscillation or at 0·005 sec. (With these values we find that $T = 23$ dimensionless time units.) The energy increase in the secondary disturbance at any time during the shear development is, by equation (2.15) *et seq.*,

$$\mathrm{E} = \mathrm{E}_0 e^{\frac{1}{2}\sigma t^2/T}, \tag{3.1}$$

so that at $t = T$,

$$\mathrm{E} \sim 100\mathrm{E}_0.$$

The energy gain of the secondary disturbance is 100-fold (a 10-fold increase in amplitude) within 0·005 sec; a dramatic increase in a relatively short time. The wave-number corresponding to this maximum gain is the value appropriate to the Rayleigh problem

$$k = \alpha h(0) = 0{\cdot}4,$$
$$\alpha = 6{\cdot}67\,\text{cm}^{-1}.$$

This value is approximately five times the wave-number of the primary disturbance ($1{\cdot}4\,\text{cm}^{-1}$) based on the propagation velocity, $c \simeq 0{\cdot}4U_f$.

The simplest model yields results in essential agreement with experiment. Intense amplification of high-frequency oscillations (short wavelength) is observed in a very short time interval.

Rather than elaborate upon the comparison of theory with experiment at this time, it is preferable first to complete the discussion of other pertinent models. These include a quasi-stationary calculation and an oscillatory simple shear simulation in which both shear strength and thickness vary with time. These models were discussed in the preceding section and it remains only to apply the results to the particular configuration, i.e. to model the free shear layers as closely as possible to the boundary-layer profiles. Finally, a more realistic model based on a time-dependent simulation of the actual boundary-layer profile is considered and the results compared to the foregoing.

Henceforth, it is desirable to change the basis of our reference quantities so that

$$U(0) = U_f, \quad h(0) = \delta,$$

for these characteristic values are more appropriate to a boundary-layer simulation. The relationship between this system and that used previously is rather elementary.

The quasi-stationary approach is based on the formula

$$\mathrm{E} = \mathrm{E}_0 \exp 2I(t),$$

with

$$I(t) = \int_0^t \frac{\eta(t)}{\xi(t)}\,\sigma(t)\,dt,$$

$$\sigma(t) = Re\{k\xi[F(k\xi)\,G(k\xi)]^{\frac{1}{2}}\}.$$

If (ξ_i, η_i) and (ξ_f, η_f) denote the initial and final values of shear thickness and strength, then we use the approximation

$$\xi = \xi_i + (\xi_f - \xi_i)\,t/T,$$
$$\eta = \eta_i + (\eta_f - \eta_i)\,t/T,$$

in order to evaluate the integral I. Furthermore, the amplification factor is also replaced by

$$\sigma(z) = Az(1 - z/z_0)\,(1 + bz) \quad (z \leqslant z_0),$$
$$= 0 \qquad\qquad\qquad\qquad (z \geqslant z_0),$$

where $\sigma'(0{\cdot}4) = 0$, $\sigma(0{\cdot}4) = 0{\cdot}2$, $z_0 = 0{\cdot}64$. In particular, we take $T = 9{\cdot}16$, $\eta_i = 0$, $\xi_i = 0{\cdot}2$, $\eta_f = 0{\cdot}25$, $\xi_f = 0{\cdot}05$ so that $b = 5$, $A = \frac{4}{9}$. For these values and the specific choice $k = 4$, we find that

$$I = \tfrac{1}{252}[1{\cdot}67(t^3 - (2{\cdot}44)^3) - 0{\cdot}082(t^4 - (2{\cdot}44)^4)].$$

The energy determined in this approximate fashion is shown in figure 7 as a function of time. It should be noted that there are serious difficulties in this approach, which we shall not discuss at this time.

The oscillatory simple shear simulation is based upon the profile

$$\left.\begin{aligned} \xi &= 0{\cdot}125 + 0{\cdot}075 \sin 2\pi t/T, \\ \eta &= 0{\cdot}125(10 - \cos 2\pi t/T), \\ T &= 18{\cdot}33. \end{aligned}\right\} \tag{3.2}$$

Here for the first time, we allow for the selection of the wave-number corresponding to maximum amplification by the time variation of shear thickness.

The numerical integration is again over a half period. The results are so similar to those shown in figure 6 that they are omitted here. It is seen that the wave-number of the most amplified mode shifts to the right during the process. The 'peak' value of k at the end of the half period lies between 4·5 and 5·0 (7·5 cm^{-1} and 8·33 cm^{-1}); the corresponding Rayleigh value in these units is 4 (6·67 cm^{-1}). The shift amounts to a change of about 15 to 25 %. The wave-number of the secondary disturbances is five to six times that of the primary oscillation (1·4 cm^{-1}).

Especially noteworthy is the fact that significant amplification of the energy in the final 'peak' mode does not occur until one-quarter of the period elapses. Therefore the principal changes take place in only one quarter period of the primary oscillation—a very short time indeed. The disturbance energy increases by two orders of magnitude (between 100 and 500 times) by the time breakdown is observed, $9 \leqslant t \leqslant 10$. Of course, since the theory is linear, these amplifications are only indicative of substantial changes in the flow.

Thus far the modes have been based upon free shear-layer approximation. Although these models are directly relevant to the problem of boundary-layer transition, there are certain refinements that are desirable. For example, we should compute the effects of the wall at $y = 0$; it turns out that since the shear-layer thickness is much smaller than its distance from the wall, the modifications are rather unimportant. Of more interest is the fact that the shear-layer models are always unstable configurations. It is important in the boundary layer to trace the instability associated with the formation of this internal shear layer starting with a neutrally stable flow. Again it is always desirable to refine the analysis by using a more realistic profile. It must be noted, however, that the main results of this more exact analysis are very similar with those obtained using the oscillatory simple shear simulation.

We consider a model consisting of four straight lines to simulate the basic flow. The profile is used as an approximation to Kovasznay's measurements (figure 4)

$$\bar{u}(y,t) = \begin{cases} 1, & 1 < y, \\ \eta + \dfrac{1-\eta}{1-\zeta}(y-\zeta), & \zeta < y < 1, \\ \mu + \dfrac{\eta-\mu}{\zeta-l}(y-l), & l < y < \zeta, \\ \dfrac{\mu}{l} y, & 0 < y < l, \end{cases} \tag{3.3}$$

where dimensionless variables are based on the free-stream velocity and boundary-layer thickness as velocity and length scales. It will be supposed that μ and l are constants but η and ζ are known functions of time. (In particular our interest centres on the case in which they are periodic functions of time.)

The stability problem requires the solution of

$$\left(\frac{\partial}{\partial t} + ik\bar{u}\right)\left(\frac{\partial^2}{\partial y^2} - k^2\right)\phi - ik\bar{u}_{yy}\phi = 0, \tag{3.4}$$

where $\bar{u}$ is defined by equation (3.3). The boundary conditions are

$$\left.\begin{aligned} \phi(0,t) &= 0, \\ \lim_{y\to\infty}\phi(y,t) &= 0, \end{aligned}\right\} \tag{3.5}$$

with the jump conditions

$$[\phi]_y = 0, \quad \left[\left(\frac{\partial}{\partial t}+ik\bar{u}\right)\phi_y - ik\phi\bar{u}_y\right]_y = 0, \tag{3.6}$$

where $y = l, \zeta, 1$ (in the notation used in § 2).

To solve equation (3.4) subject to the conditions (3.5) we take

$$\phi = \left\{\begin{aligned} &d\,e^{-ky}, && 1 < y, \\ &a\cosh ky + b\sinh ky, && \zeta < y < 1, \\ &g\cosh ky + h\sinh ky, && l < y < \zeta, \\ &e\sinh ky, && 0 < y < l. \end{aligned}\right\} \tag{3.7}$$

The jump conditions (3.6) then yield six equations for the six unknown functions a, b, d, e, g, h. In practice it was found convenient to work with four linear combinations, namely, A, B, C, D; where

$$\left.\begin{aligned} a &= e^{-k}A + e^{k}B, \\ b &= e^{-k}A - e^{k}B, \\ g &= e^{k}C, \\ h &= e^{k}D. \end{aligned}\right\} \tag{3.8}$$

The three differential equations governing the motion are found to be

$$\frac{dA}{dt} = iA\left[-k+\frac{1}{2}\frac{1-\eta}{1-\zeta}\right] + \tfrac{1}{2}iB\frac{1-\eta}{1-\zeta}, \tag{3.9}$$

$$\begin{aligned} \frac{dB}{dt} = iA\Bigg[&k(1-\eta)\,e^{-2k} - \frac{1}{2}\left(\frac{1-\eta}{1-\zeta}\right)e^{-2k} - ik\frac{d\zeta}{dt}e^{-2k}\coth k\zeta \\ &+\left(\frac{\mu}{l}-\frac{\eta-\mu}{\zeta-l}\right)e^{-2k}(1+\coth k\zeta)\sinh^2 kl - \left(\frac{1-\eta}{1-\zeta}-\frac{\eta-\mu}{\zeta-l}\right)e^{-2k}e^{k\zeta}\sinh k\zeta\Bigg] \\ &+iB\Bigg[-k\eta - \frac{1}{2}\left(\frac{1-\eta}{1-\zeta}\right)e^{-2k} - ik\frac{d\zeta}{dt}\coth k\zeta \\ &-\left(\frac{\mu}{l}-\frac{\eta-\mu}{\zeta-l}\right)(1-\coth k\zeta)\sinh^2 kl - \left(\frac{1-\eta}{1-\zeta}-\frac{\eta-\mu}{\zeta-l}\right)e^{-k\zeta}\sinh k\zeta\Bigg] \\ &+iC\left[k(\eta-\mu)+ik\frac{d\zeta}{dt}\coth k\zeta + \left(\frac{\mu}{l}-\frac{\eta-\mu}{\zeta-l}\right)\frac{\sinh kl\sinh k(\zeta-l)}{\sinh k\zeta}\right], \end{aligned} \tag{3.10}$$

$$\begin{aligned} \frac{dC}{dt} = iA&\left[\left(\frac{\mu}{l}-\frac{\eta-\mu}{\zeta-l}\right)e^{-2k}(1+\coth k\zeta)\sinh^2 kl\right] \\ &-iB\left[\left(\frac{\mu}{l}-\frac{\eta-\mu}{\zeta-l}\right)(1-\coth k\zeta)\sinh^2 kl\right] \\ &+iC\left[-k\mu+\left(\frac{\mu}{l}-\frac{\eta-\mu}{\zeta-l}\right)\frac{\sinh kl\sinh k(\zeta-l)}{\sinh k\zeta}\right], \end{aligned} \tag{3.11}$$

$$D = A(1+\coth k\zeta)\,e^{-2k} - B(1-\coth k\zeta) - C\coth k\zeta. \tag{3.12}$$

The total energy in the disturbance is

$$\mathrm{E}(t) = 2\pi k \int_0^\infty \left(|\phi|^2 + \frac{1}{k^2} |\phi_y|^2 \right) dy, \tag{3.13}$$

and the component energies in the various layers are given by,

$$\left.\begin{aligned} \mathrm{E}_1(t) &= 2\pi k \int_1^\infty I\, dy, \\ \mathrm{E}_2(t) &= 2\pi k \int_\zeta^1 I\, dy, \\ \mathrm{E}_3(t) &= 2\pi k \int_l^\zeta I\, dy, \\ \mathrm{E}_4(t) &= 2\pi k \int_0^l I\, dy, \\ I &= |\phi|^2 + 1/k^2 |\phi_y|^2. \end{aligned}\right\} \tag{3.14}$$

Clearly

$$\mathrm{E} = \sum_1^4 \mathrm{E}_i. \tag{3.15}$$

A little algebra shows that

$$\begin{aligned} \mathrm{E}(t) \propto\ & e^{-2k}[1 + e^{-2k}(1 - e^{-2k\zeta})^{-1}] AA^* \\ & + e^{-2k\zeta}(1 - e^{-2k\zeta})^{-1} BB^* + e^{-2k}(1 - e^{-2k\zeta})^{-1}(AB^* + A^*B) \\ & + \tfrac{1}{2}[(1 + e^{-2kl})(1 - e^{-2kl})^{-1} - (1 + e^{-2k\zeta})(1 - e^{-2k\zeta})^{-1}] CC^*, \end{aligned} \tag{3.16}$$

$$\mathrm{E}_1(t) \propto AA^* + BB^* + AB^* + A^*B, \tag{3.17}$$

$$\mathrm{E}_2(t) \propto (1 - e^{-2k(1-\zeta)})(e^{-2k} AA^* + e^{-2k\zeta} BB^*), \tag{3.18}$$

$$\begin{aligned} \mathrm{E}_3(t) \propto\ & e^{2k\zeta}[(1 - e^{-4k\zeta} - e^{-2k(\zeta-l)} - e^{-2k(\zeta+l)})(CC^* + DD^*) \\ & + (1 + e^{-4k\zeta} - e^{-2k(\zeta-l)} - e^{-2k(\zeta+l)})(CD^* + C^*D)], \end{aligned} \tag{3.19}$$

$$\mathrm{E}_4(t) \propto (1 + e^{-2kl})^2 CC^* + (1 - e^{-2kl})^2 DD^* + (1 - e^{-4kl})(CD^* + C^*D). \tag{3.20}$$

Here $\mathrm{E}(t)/\mathrm{E}(0)$ is a measure of the instability, and $\mathrm{E}_i(t)/\mathrm{E}(0)$ gives a measure of the amplitude concentration in y.

Our interest lies in the case when η and ζ are periodic functions of time; over one half period the profile $\bar{u}(y, t)$ goes from something approximating a Blasius profile to one approximating a shear profile well out in the boundary layer. On a quasi-steady basis the first profile shown in figure 4 would be neutral; the equations (3.9)–(3.19) having solutions proportional to $e^{-i\omega t}$ with three values of ω all real. However, in the same way, the third profile ($t/T = 0{\cdot}38$) of figure 4 would exhibit an inflexional instability, resulting in two of the ω's being complex conjugates and remaining one real. Therefore, over one half cycle of the primary wave, the local flow characteristics can give rise to a strong instability associated with the formation of the shear layer. At time $t = 0$, using $\eta(0)$ and $\zeta(0)$, there are three values of ω ($\omega^{(c)} < \omega^{(b)} < \omega^{(a)}$) which were found for given values of the wave-number k, as were the corresponding initial values of the eigenfunctions for each case. (In other words, we assume $\eta(t) = \eta(0)$, $\zeta(t) = \zeta(0)$ for $t \leqslant 0$.) With these initial values the equations were then integrated using a fourth-order Runge–Kutta method, and the corresponding energy ratios calculated. These are shown

in figures 5 and 6. The superscripts correspond to the three cases. It was found that the initial conditions corresponding to mode '*b*' produced the largest energy gains, although mode '*a*' was also strong (figure 5(*a*)); mode '*c*' was comparatively weak and is omitted in the diagrams. In all calculations we took

$$\mu = 0{\cdot}4,$$
$$l = 0{\cdot}22,$$
$$\eta = 0{\cdot}70 + 0{\cdot}20\cos(2\pi t/18{\cdot}33),$$
$$\zeta = 0{\cdot}75 - 0{\cdot}15\cos(2\pi t/18{\cdot}33),$$

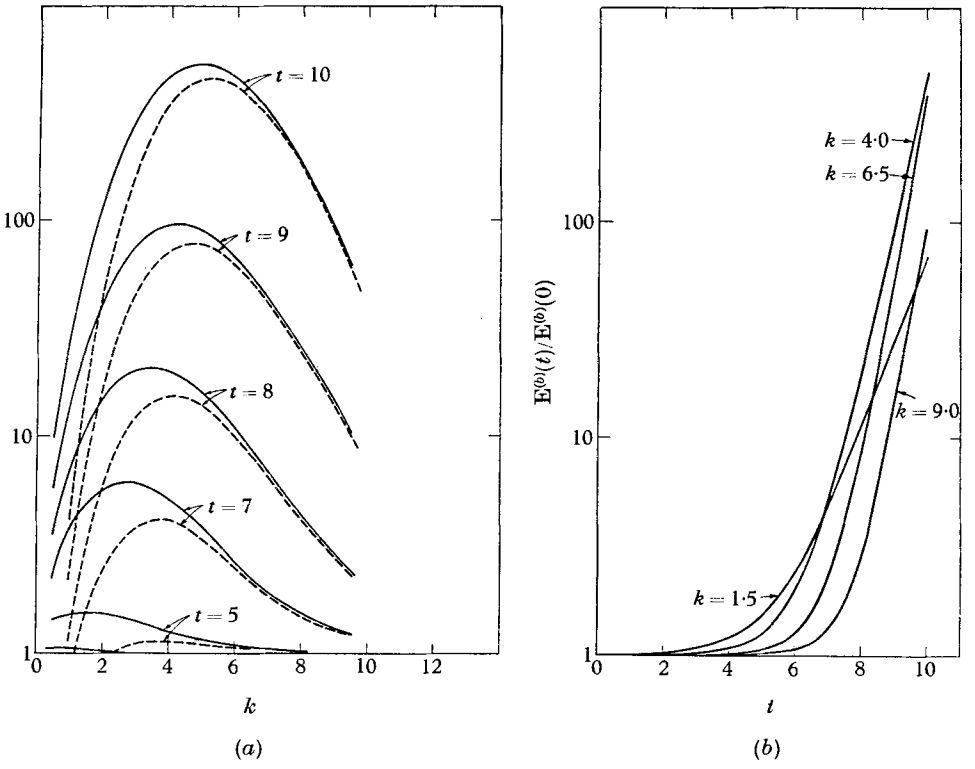

FIGURE 5. (*a*) $E^{(a)}(t)/E^{(a)}(0)$ (----), $E^{(b)}(t)/E^{(b)}(0)$ (——), as functions of k for various times t, in boundary-layer simulation. (*b*) $E^{(b)}(t)/E^{(b)}(0)$ as a function of t for various wave-numbers k; $\mu = 0{\cdot}4$, $l = 0{\cdot}22$, $\eta = 0{\cdot}70 + 0{\cdot}20\cos 2\pi t/T$, $\zeta = 0{\cdot}75 - 0{\cdot}15\cos 2\pi t/T$; $T = 18{\cdot}33$.

which yield a reasonable straight-line approximation to the profile measured by Kovasznay *et al.* In particular, the shear strength and shear thickness were made to conform as closely as possible, although no variation of the shear zone with height has been incorporated.

The results clearly show the disturbance energy to peak strongly near $k = 5$ in one half cycle of the primary wave. The wave-number corresponding to peak excitation shifts to higher values as the shear layer collapses (wave-number selection). The principal amplification occurs only over the quarter cycle preceding breakdown. The amplitude gain is one order of magnitude, the energy gain at least two orders.

The energy in the disturbance is concentrated mainly in the shear zone; the wall produces little effect on the stability characteristics. It is not surprising then that the oscillatory simple shear simulation provides almost identical results with the more exact boundary-layer model. This is illustrated in figure 7 which

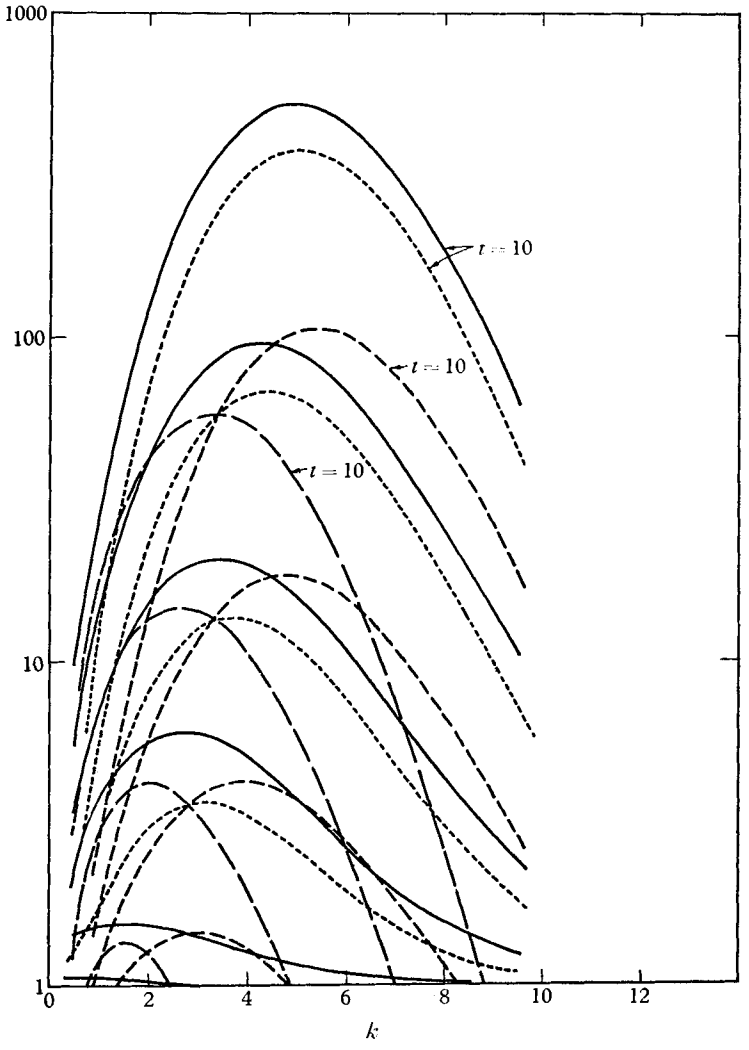

FIGURE 6. $E^{(b)}(t)/E^{(b)}(0)$ (——), $E_1^{(b)}(t)/E^{(b)}(0)$ (– – –), $E_2^{(b)}(t)/E^{(b)}(0)$ (– – –), $E_3^{(b)}(t)/E^{(b)}(0)$ (– – –), as functions of k for various times t. Time $t = 10$ is indicated. Each energy ratio is shown at $t = 9$, 8, 7 and (for $E^{(b)}/E^{(b)}(0)$) at $t = 5$, 2.

presents $E(t)/E(0)$ versus time for the particular mode $k = 4$, as determined by each of the four models; simple shear, quasi-steady, oscillatory simple shear, boundary-layer simulation. The comparison implies that the significant amplification occurs in a shorter time interval for those cases involving a variable shear thickness. The more realistic models lead to peak amplification of higher wave-number modes in a shorter time interval.

These calculations are a strong indication that the secondary instabilities on the modified boundary-layer flow are indeed a mechanism for the sudden amplification of high-frequency disturbances.

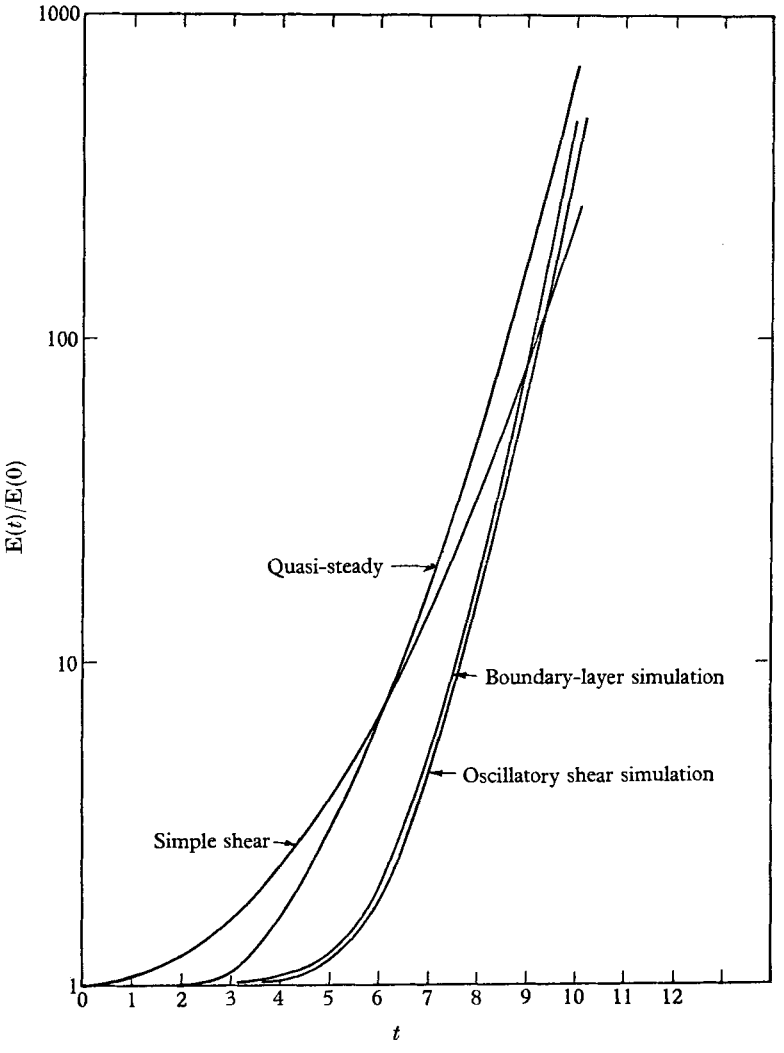

FIGURE 7. E(t)/E(0) for $k = 4$ comparing results of four theories; boundary-layer simulation, oscillatory shear simulation, quasi-steady, and simple shear models.

4. Conclusion

The investigation of the preceding section utilizes simple models of the basic flow as modified by the primary oscillations in order to determine the stability characteristics of the secondary disturbances. The analysis is linear but the growth rates are such that the tendency toward a violent instability is conclusive. A finite amplitude inviscid analysis of the steady shear layer discussed in § 2 shows that the first Landau constant is a pure imaginary. To this order then

there is no tendency for the growth rate to be modified, but only a dependence of frequency on amplitude.

We have found that over one half cycle of the primary wave the amplitude of the most unstable secondary wave will increase by a factor of the order of 10, its energy by a factor of 100 or more. The wavelength of the secondary instability corresponding to maximum gain is about one-fifth that of the primary oscillation corresponding to an instability with frequency about eight times that of the primary wave. The contraction process acts as a frequency selector and an amplifier. Thus a theory based on a local secondary instability of the shear layer is in reasonable agreement with the breakdown measurements of Klebanoff and Kovasznay. The development of the observed 'spikes' is doubtless largely governed by three-dimensional and non-linear effects, but their formation is explainable by the ideas proposed here.

A simple picture of this process is the continuous creation of local instabilities (leading to the birth of turbulent spots) at favourable positions and times corresponding to the most intense shear layer. At a fixed position optimum conditions will occur once each cycle of the primary wave. This new instability will be convected downstream with a speed c_2 (corresponding to the local inflexional speed); c_2 being approximately twice the speed c_1 of the primary wave. This idealization is conveniently represented in an (x, t)-plane as indicated in figure 8; here $x = 0$ represents the position of the onset of the secondary instability and λ_1 the wavelength of the primary oscillation. Measurements made just beyond $x = 0$ should show bursts of the new instability, again consistent with the experiments. Alternatively, this process can be considered as an eddy-shedding mechanism relative to an observer moving with the wave, as has been suggested by Klebanoff (1962).

The simple qualitative picture we propose can be summarized as follows. The strong three-dimensional features of the initial instability tend to 'soften up' local spanwise positions for the occurrence of a violent secondary instability of the Helmholtz type. It may well be that a purely two-dimensional disturbance alone can produce this shear layer if its amplitude is large enough; but the inevitable three dimensionality accelerates its development in particular with respect to its position relative to the wall. In natural transition, where the three dimensionality is not as organized as in the controlled case one would expect the primary instability to be longer in extent and the breakdown to occur at less regular spanwise positions. It may be conjectured that high instabilities corresponding to the breakdown of local vortex sheets can give rise to shorter length scales in a similar manner, as a cascade-type process.

The recent experiments of Sato & Kuriki (1961) on the instability of the laminar wake show the breakdown process to be much less violent. This is not surprising in view of the fact that while any local shears produced by the secondary flow may give rise to short length scale instabilities their growth rates are determined by the maximum local shear. Any secondary instability arising will therefore be governed by a geometry similar to that of the primary instability and their growth rates can be expected to be comparable. In the case of the boundary layer, the primary and secondary instabilities develop from very different geometries

and their growth rates are by no means comparable. Also it should be noted that the wake is a case of an expanding layer and hence the longer primary waves tend to be accentuated.

Finally, we would again stress that the models investigated are simplified flows which exhibit only the dominant features of the observed flow at break-

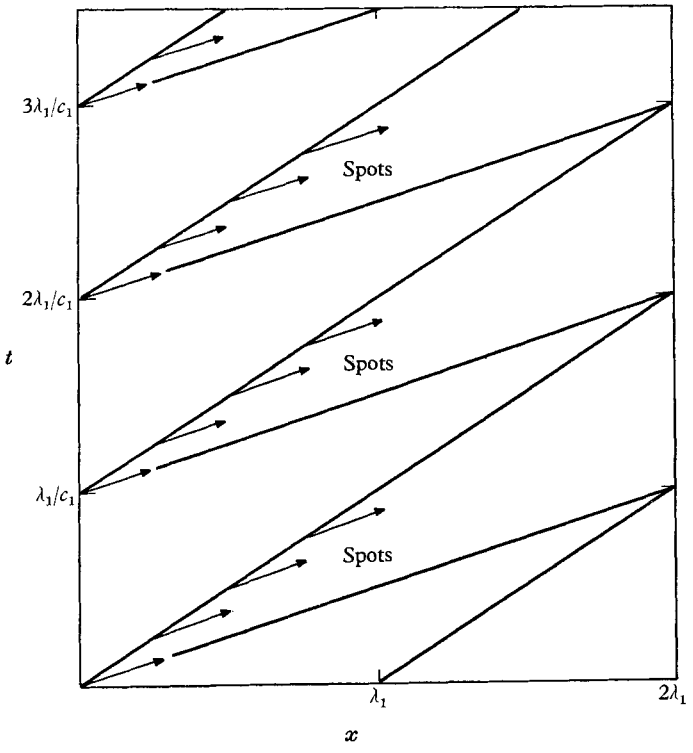

FIGURE 8. (x, t) representation showing favourable locations for onset of secondary instability.

down. There are many improvements that should be included to give a better description; in particular that the development is really space-like rather than time-like. The above analysis is an attempt to give a simple theoretical explanation of what must be a very complicated physical situation.

This research was jointly supported by the U.S. Air Force, Contract AF 49(638)-708 and the Office of Naval Research, Contract Nonr-1841(12); the calculations were performed at the M.I.T. Computation Center.

The authors wish to acknowledge the stimulation afforded this research by their close continued association with Professor C. C. Lin.

REFERENCES

BENNEY, D. J. 1961 *J. Fluid Mech.* **10**, 209.

BENNEY, D. J. & LIN, C. C. 1960 *Phys. Fluids*, **3**, 656.

CARRIER, G. F. 1954 Los Alamos Internal Report.

ESCH, R. E. 1957 *J. Fluid Mech.* **3**, 289.

KLEBANOFF, P. D., TIDSTROM, D. D. & SARGENT, L. M. 1962 *J. Fluid Mech.* **12**, 1.

KOVASZNAY, L. S. G., KOMODA, H. & VASUDEVA, B. R. 1962 *Report:* The Johns Hopkins University, Baltimore.

LIN, C. C. 1945 Parts I, II, III. *Quart. Appl. Math.* **3**, 117, 218, 277.

LIN, C. C. 1955 *Hydrodynamic Stability*. Cambridge University Press.

SCHUBAUER, G. B. 1957 *Boundary Layer Research Symposium*, p. 85. Freiburg.

SCHUBAUER, G. B. & SKRAMSTEAD, H. K. 1948 *Nat. Adv. Comm. Aero., Wash., Report*, no. 909.

SATO, H. & KURIKI, K. 1961 *J. Fluid Mech.* **11**, 321.

STUART, J. T. 1960 *J. Fluid Mech.* **9**, 353.

WATSON, J. 1960 *J. Fluid Mech.* **9**, 371.